Progress In Electromagnetics Research, Vol. 129, 197–214, 2012

A GENERALIZED COUPLED-LINE DUAL-BAND WILKINSON POWER DIVIDER WITH EXTENDED PORTS

J. C. Li*, Y. L. Wu, Y. A. Liu, J. Y. Shen, S. L. Li, and C. P. Yu

School of Electronic Engineering, Beijing University of Posts and Telecommunications, Beijing, China

Abstract—A generalized two-way coupled-line power divider with extended ports for dual band is proposed in this paper. The power divider is composed of two section coupled-lines, one conventional transmission line, and an isolation resistor, and employs extension of a transmission line or coupled-line at each port. The design equations are obtained based on even- and odd-mode analysis, and analytical ideal closed-form scattering parameter expressions derived. Because the traditional ring structure is a special case of coupled line, four cases of this generalized power divider are discussed and compared. In addition, the six power dividers simulated results of three special cases are shown. Finally, three fabricated power dividers measurements are used to certify this proposed structure and corresponding design parameters.

1. INTRODUCTION

Power dividers are well-known three-port devices, and very important for microwave and millimeter-wave systems, which can be widely used in balanced power amplifier, radar system, feeding networks for antenna arrays, measurement systems, mixers and phase shifters etc.. As is well known, the original power divider developed by Wilkinson [1] consists of two quarter-wavelength lines and operates in a single band. Rapid developments in modern wireless communication have imposed their components to operate at dual-band and multiple bands. The corresponding dual-frequency power divider with analytical design

Received 9 May 2012, Accepted 13 June 2012, Scheduled 19 June 2012

* Corresponding author: Jiu Chao Li (lijiuchao@gmail.com).

method was developed after Dr. Monzon derived the closed-form design equations for the dual frequency impedance transformer [2], and various novel structures have been proposed in [3–23, 32]. To satisfy the ideal isolation and improve the matching characteristics, new isolation structures including parallel RLC and series RLC are proposed in [3–6]. The papers [7–10] introduce modified impedance matching structure, and the dual-band power dividers are presented in [11, 12] without reactive components, N-way and multi-way dual-band planar power dividers are discussed in [14–19]. In order to reach high power combining application, the paper [21] presented dual-band unequal Gysel power divider with arbitrary termination resistance. However, the proposed power divider was only for dual-band applications. In [22, 23], the novel methods are presented for the design of multi-band power dividers. After decreasing the inherent circuit size of the conventional Wilkinson power divider and to develop high performance power dividers, coupled-line sections are used to design power divider [24–31]. The power divider given in [24] is single-band design, and provides more freedom of design parameters. The dual-band power divider two-section cascaded coupled-line structure in [25] has small frequency-ratio limitation, but frequency-ratio limitation of the dual-band divider is improved in [26]. It is necessary to point out that these coupled-line power dividers are one form of the structure in [27]. Obviously, the coupled-line dual-band power divider has compact size. In addition, other coupled-line power dividers are studied in [28–31].

In this paper, a generalized coupled-line two-way power divider with extended ports for dual band is proposed, which has two section coupled-lines, one conventional transmission line, and one isolation resistor. The coupled-line has compact structure and flexible design parameters due to the introduction of even- and odd-mode impedances. Based on the even- and odd-mode analysis, rigorous design equations and analytical ideal closed-form scattering parameter expressions are derived. The design parameters can be calculated by solving nonlinear design equations which are obtained by the conventional even- and odd-mode analysis. Since the traditional transmission line is a special case of coupled line, four cases of this generalized power divider are discussed and compared. In addition, the simulated results of three special cases are shown and three fabricated power dividers certify this proposed structure and corresponding design parameters. This paper can be considered as an extension of the Wilkinson power divider [9].

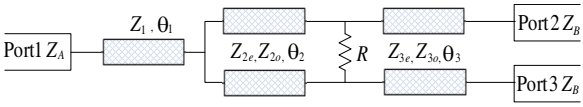

Figure 1. Proposed generalized coupled-line dual-band two-way Wilkinson power divider.

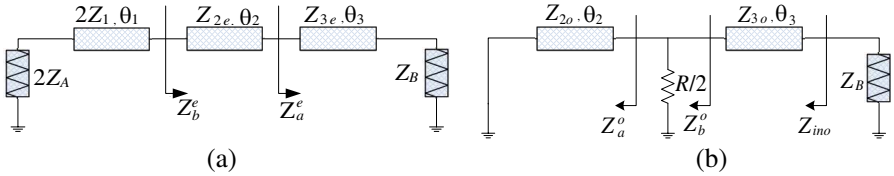

Figure 2. The equivalent circuits for (a) the even-mode analysis and (b) the odd-mode analysis.

2. CIRCUIT STRUCTURES AND DESIGN THEORY

Figure 1 illustrates the basic circuit structure of the proposed coupled-line power divider with extended ports. The structure includes two section coupled-lines, one conventional transmission line, and one isolation resistor. Without loss of generality, the port 1 connects impedance Z_A while the output ports 2 and 3 connect impedance Z_B. The microstrip transmission line with characteristic Z_1 and electrical length θ_1, these coupled lines impedances Z_{ie} and Z_{io}, and electrical length θ_i, where $i = 1, 2$, the isolation structure consists of a lumped resistor R.

2.1. Analytical Nonlinear Equations for Parameters Design

An ideal equal dual-band power divider should satisfy that all ports are matched and two output ports (Port 2 and Port 3 shown in Figure 1) are isolated perfectly. After applying the even- and odd-mode analysis, the following relationship of the parameters in Figure 2(a) must be satisfied:

$$Z_a^e = \frac{Z_{3e}\left(Z_B + jZ_{3e}\tan\theta_3\right)}{Z_{3e} + jZ_B\tan\theta_3} \tag{1}$$

$$Z_b^e = \frac{Z_{2e}\left(Z_a^e + jZ_{2e}\tan\theta_2\right)}{Z_{2e} + jZ_a^e\tan\theta_2} \tag{2}$$

$$2Z_A = \frac{2Z_1\left(Z_b^e + j2Z_1\tan\theta_1\right)}{2Z_1 + jZ_b^e\tan\theta_1} \tag{3}$$

After several algebraic operations, the real and imaginary parts are expressed as:

$$(2Z_A - Z_B) Z_1 Z_{2e} Z_{3e} + \left(2Z_B Z_1^2 - Z_A Z_{2e}^2\right) Z_{3e} \tan\theta_1 \tan\theta_2 + \left(2Z_B Z_1^2 - Z_A Z_{3e}^2\right) Z_{2e} \tan\theta_1 \tan\theta_3 + \left(2Z_B Z_{2e}^2 - 2Z_A Z_{3e}^2\right) Z_1 \tan\theta_2 \tan\theta_3 = 0 \quad (4)$$

$$\left(2Z_1^2 Z_{3e}^2 - Z_A Z_B Z_{2e}^2\right) \tan\theta_1 \tan\theta_2 \tan\theta_3 + \left(Z_A Z_B - 2Z_1^2\right) Z_{2e} Z_{3e} \tan\theta_1 + \left(2Z_A Z_B - Z_{2e}^2\right) Z_1 Z_{3e} \tan\theta_2 + \left(2Z_A Z_B - Z_{3e}^2\right) Z_1 Z_{2e} \tan\theta_3 = 0 \quad (5)$$

Similarly, from Figure 2(b), the following equations including the isolated resistor can be written as:

$$Z_a^o = jZ_{2o} \tan\theta_2 \quad (6)$$

$$Z_b^o = \frac{Z_a^o \cdot \frac{R}{2}}{Z_a^o + \frac{R}{2}} = \frac{Z_a^o R}{2Z_a^o + R} \quad (7)$$

$$Z_{ino} = \frac{Z_{3o}\left(Z_b^o + jZ_{3o} \tan\theta_3\right)}{Z_{3o} + jZ_b^o \tan\theta_3} = Z_B \quad (8)$$

Using (6), (7), and (8), the real and imaginary parts can be obtained as follows:

$$\left(Z_B R - 2Z_{3o}^2\right) Z_{2o} \tan\theta_2 \tan\theta_3 - Z_B Z_{3o} R = 0 \quad (9)$$

$$RZ_{3o} \tan\theta_3 - (2Z_B - R) Z_{2o} \tan\theta_2 = 0 \quad (10)$$

Once the terminal impedances Z_A, Z_B, Z_C and the electrical lengths θ_1, θ_2 and θ_3 are determined, optimization algorithms are then used to obtain the final desired values, such as Z_1, Z_{2e}, Z_{2o}, Z_{3e}, Z_{3o} and R can be obtained according to the analytical design Equations (4), (5) and (9), (10).

$$\begin{cases} S_{12} = S_{21} = S_{13} = S_{31} \\ S_{22} = S_{33} \\ S_{23} = S_{32} \\ S_{11} = S_{11e} \\ S_{21} = \dfrac{S_{21e}}{\sqrt{2}} \\ S_{22} = \dfrac{S_{22e} + S_{22o}}{2} \\ S_{32} = \dfrac{S_{22e} - S_{22o}}{2} \end{cases} \quad (11)$$

2.2. Analytical Ideal Scattering Parameters

In order to improve the power dividers designing, it is necessary to study the theoretical scattering parameters of the generalized power divider. Due to symmetry of the circuit shown in Figure 1, the relationship (11) must be satisfied [27]. So, we only need to obtain the scattering parameters S_{11e}, S_{21e}, S_{22e} and S_{22o}, we will know the ideal-closed form equations for scattering parameters. The even-mode $ABCD$-matrix between two ports (Port 1 and Port 2) is expressed from Figure 2(a) as follow (12):

$$\begin{aligned}
&\begin{bmatrix} A_{12} & B_{12} \\ C_{12} & D_{12} \end{bmatrix}_e \\
&= \begin{bmatrix} \cos\theta_1 & j2Z_1\sin\theta_1 \\ j\frac{1}{2Z_1}\sin\theta_1 & \cos\theta_1 \end{bmatrix} \begin{bmatrix} \cos\theta_2 & jZ_{2e}\sin\theta_2 \\ j\frac{1}{Z_{2e}}\sin\theta_2 & \cos\theta_2 \end{bmatrix} \begin{bmatrix} \cos\theta_3 & jZ_{3e}\sin\theta_3 \\ j\frac{1}{Z_{3e}}\sin\theta_3 & \cos\theta_3 \end{bmatrix} \\
&= \begin{bmatrix} \dfrac{\begin{pmatrix} \cos\theta_1\cos\theta_2\cos\theta_3 Z_{2e}Z_{3e} \\ -2Z_1Z_{3e}\sin\theta_1\sin\theta_2\cos\theta_3 \\ -Z_{2e}^2\sin\theta_2\sin\theta_3\cos\theta_1 \\ -2Z_1Z_{2e}\sin\theta_1\cos\theta_2\sin\theta_3 \end{pmatrix}}{Z_{2e}Z_{3e}} & \dfrac{j\begin{pmatrix} \cos\theta_1\cos\theta_2\sin\theta_3 Z_{2e}Z_{3e} \\ -2Z_1Z_{3e}\sin\theta_1\sin\theta_2\sin\theta_3 \\ +Z_{2e}^2\sin\theta_2\cos\theta_1\cos\theta_3 \\ +2Z_1Z_{2e}\sin\theta_1\cos\theta_2\cos\theta_3 \end{pmatrix}}{Z_{2e}} \\ \dfrac{j\begin{pmatrix} Z_{2e}Z_{3e}\sin\theta_1\cos\theta_2\cos\theta_3 \\ +2Z_1Z_{3e}\sin\theta_2\cos\theta_1\cos\theta_3 \\ +2Z_1Z_{2e}\cos\theta_1\cos\theta_2\sin\theta_3 \\ -Z_{2e}^2\sin\theta_1\sin\theta_2\sin\theta_3 \end{pmatrix}}{2Z_1Z_{2e}Z_{3e}} & \dfrac{\begin{pmatrix} 2Z_1Z_{2e}\cos\theta_1\cos\theta_2\cos\theta_3 \\ -Z_{2e}^2\sin\theta_1\sin\theta_2\cos\theta_3 \\ -Z_{2e}Z_{3e}\sin\theta_1\cos\theta_2\sin\theta_3 \\ -2Z_1Z_{3e}\sin\theta_2\sin\theta_3\cos\theta_1 \end{pmatrix}}{2Z_1Z_{2e}} \end{bmatrix}
\end{aligned} \tag{12}$$

Similarly, from Figure 2(b), the odd-mode $ABCD$-matrix can be obtained as following (13):

$$\begin{aligned}
&\begin{bmatrix} A_{12} & B_{12} \\ C_{12} & D_{12} \end{bmatrix}_o = \begin{bmatrix} \cos\theta_2 & jZ_{2o}\sin\theta_2 \\ j\frac{1}{Z_{2o}}\sin\theta_2 & \cos\theta_2 \end{bmatrix} \begin{bmatrix} 1 & 0 \\ \frac{2}{R} & 1 \end{bmatrix} \begin{bmatrix} \cos\theta_3 & jZ_{3o}\sin\theta_3 \\ j\frac{1}{Z_{3o}}\sin\theta_3 & \cos\theta_3 \end{bmatrix} \\
&= \begin{bmatrix} \dfrac{\begin{pmatrix} j2Z_{2o}Z_{3o}\sin\theta_2\cos\theta_3 \\ +R\left(Z_{3o}\cos\theta_2\cos\theta_3 \right. \\ \left. -Z_{2o}\sin\theta_2\sin\theta_3\right) \end{pmatrix}}{RZ_{3o}} & \dfrac{\begin{pmatrix} jR\left(Z_{3o}\cos\theta_2\sin\theta_3 \right. \\ \left. +Z_{2o}\sin\theta_2\cos\theta_3\right) \\ -2Z_{2o}Z_{3o}\sin\theta_2\sin\theta_3 \end{pmatrix}}{R} \\ \dfrac{\begin{pmatrix} jR\left(Z_{3o}\sin\theta_2\cos\theta_3 \right. \\ \left. +Z_{2o}\cos\theta_2\sin\theta_3\right) \\ +2Z_{2o}Z_{3o}\cos\theta_2\cos\theta_3 \end{pmatrix}}{RZ_{2o}Z_{3o}} & \dfrac{\begin{pmatrix} j2Z_{2o}Z_{3o}\cos\theta_2\sin\theta_3 \\ +R\left(Z_{2o}\cos\theta_2\cos\theta_3 \right. \\ \left. -Z_{3o}\sin\theta_2\sin\theta_3\right) \end{pmatrix}}{RZ_{2o}} \end{bmatrix}
\end{aligned} \tag{13}$$

According to the transformation between scattering parameters and $ABCD$-matrix parameters, the ideal closed-form even-mode and odd-mode S-parameters (Z_A and Z_B are real resistances) can be obtained as (14)–(17), based on combining (11) and (14)–(17), the analytical mathematical equations can obtain for the proposed generalized power

divider in Figure 1.

$$S_{11e} = \frac{\left(\begin{array}{l}(Z_B - 2Z_A)\, Z_1 Z_{2e} Z_{3e} \cos\theta_1 \cos\theta_2 \cos\theta_3 \\ + \left(Z_A Z_{2e}^2 - 2Z_B Z_1^2\right) Z_{3e} \sin\theta_1 \sin\theta_2 \cos\theta_3 \\ + \left(2Z_A Z_{3e}^2 - Z_B Z_{2e}^2\right) Z_1 \cos\theta_1 \sin\theta_2 \sin\theta_3 \\ + \left(Z_A Z_{3e}^2 - 2Z_B Z_1^2\right) Z_{2e} \sin\theta_1 \cos\theta_2 \sin\theta_3 \\ + j \left(\begin{array}{l}(Z_{2e} Z_{3e} - 2Z_A Z_B)\, Z_1 Z_{3e} \cos\theta_1 \cos\theta_2 \sin\theta_3 \\ + \left(Z_{2e}^2 Z_A Z_B - 2Z_1^2 Z_{3e}^2\right) \sin\theta_1 \sin\theta_2 \sin\theta_3 \\ + \left(Z_{2e}^2 - 2Z_A Z_B\right) Z_1 Z_{3e} \cos\theta_1 \sin\theta_2 \cos\theta_3 \\ + \left(2Z_1^2 - Z_A Z_B\right) Z_{2e} Z_{3e} \sin\theta_1 \cos\theta_2 \cos\theta_3 \end{array}\right) \end{array}\right)}{\left(\begin{array}{l}(Z_B + 2Z_A)\, Z_1 Z_{2e} Z_{3e} \cos\theta_1 \cos\theta_2 \cos\theta_3 \\ - \left(Z_A Z_{2e}^2 + 2Z_B Z_1^2\right) Z_{3e} \sin\theta_1 \sin\theta_2 \cos\theta_3 \\ - \left(2Z_A Z_{3e}^2 + Z_B Z_{2e}^2\right) Z_1 \cos\theta_1 \sin\theta_2 \sin\theta_3 \\ - \left(Z_A Z_{3e}^2 + 2Z_B Z_1^2\right) Z_{2e} \sin\theta_1 \cos\theta_2 \sin\theta_3 \\ + j \left(\begin{array}{l}(Z_{2e} Z_{3e} + 2Z_A Z_B)\, Z_1 Z_{3e} \cos\theta_1 \cos\theta_2 \sin\theta_3 \\ - \left(Z_{2e}^2 Z_A Z_B + 2Z_1^2 Z_{3e}^2\right) \sin\theta_1 \sin\theta_2 \sin\theta_3 \\ + \left(Z_{2e}^2 + 2Z_A Z_B\right) Z_1 Z_{3e} \cos\theta_1 \sin\theta_2 \cos\theta_3 \\ + \left(2Z_1^2 + Z_A Z_B\right) Z_{2e} Z_{3e} \sin\theta_1 \cos\theta_2 \cos\theta_3 \end{array}\right) \end{array}\right)} \quad (14)$$

$$S_{21e} = \frac{2Z_1 Z_{2e} Z_{3e} \sqrt{2Z_A Z_B}}{\left(\begin{array}{l}(Z_B + 2Z_A)\, Z_1 Z_{2e} Z_{3e} \cos\theta_1 \cos\theta_2 \cos\theta_3 \\ - \left(Z_A Z_{2e}^2 + 2Z_B Z_1^2\right) Z_{3e} \sin\theta_1 \sin\theta_2 \cos\theta_3 \\ - \left(2Z_A Z_{3e}^2 + Z_B Z_{2e}^2\right) Z_1 \cos\theta_1 \sin\theta_2 \sin\theta_3 \\ - \left(Z_A Z_{3e}^2 + 2Z_B Z_1^2\right) Z_{2e} \sin\theta_1 \cos\theta_2 \sin\theta_3 \\ + j \left(\begin{array}{l}(Z_{2e} Z_{3e} + 2Z_A Z_B)\, Z_1 Z_{3e} \cos\theta_1 \cos\theta_2 \sin\theta_3 \\ - \left(Z_{2e}^2 Z_A Z_B + 2Z_1^2 Z_{3e}^2\right) \sin\theta_1 \sin\theta_2 \sin\theta_3 \\ + \left(Z_{2e}^2 + 2Z_A Z_B\right) Z_1 Z_{3e} \cos\theta_1 \sin\theta_2 \cos\theta_3 \\ + \left(2Z_1^2 + Z_A Z_B\right) Z_{2e} Z_{3e} \sin\theta_1 \cos\theta_2 \cos\theta_3 \end{array}\right) \end{array}\right)} \quad (15)$$

$$S_{22e}=\frac{\left(\begin{array}{l}(2Z_A-Z_B)\,Z_1Z_{2e}Z_{3e}\cos\theta_1\cos\theta_2\cos\theta_3\\+\left(2Z_BZ_1^2-Z_AZ_{2e}^2\right)Z_{3e}\sin\theta_1\sin\theta_2\cos\theta_3\\+\left(Z_BZ_{2e}^2-2Z_AZ_{3e}^2\right)Z_1\cos\theta_1\sin\theta_2\sin\theta_3\\+\left(2Z_BZ_1^2-Z_AZ_{3e}^2\right)Z_{2e}\sin\theta_1\cos\theta_2\sin\theta_3\\+j\left(\begin{array}{l}(Z_{2e}Z_{3e}-2Z_AZ_B)\,Z_1Z_{3e}\cos\theta_1\cos\theta_2\sin\theta_3\\+\left(Z_{2e}^2Z_AZ_B-2Z_1^2Z_{3e}^2\right)\sin\theta_1\sin\theta_2\sin\theta_3\\+\left(Z_{2e}^2-2Z_AZ_B\right)Z_1Z_{3e}\cos\theta_1\sin\theta_2\cos\theta_3\\+\left(2Z_1^2-Z_AZ_B\right)Z_{2e}Z_{3e}\sin\theta_1\cos\theta_2\cos\theta_3\end{array}\right)\end{array}\right)}{\left(\begin{array}{l}(Z_B+2Z_A)\,Z_1Z_{2e}Z_{3e}\cos\theta_1\cos\theta_2\cos\theta_3\\-\left(Z_AZ_{2e}^2+2Z_BZ_1^2\right)Z_{3e}\sin\theta_1\sin\theta_2\cos\theta_3\\-\left(2Z_AZ_{3e}^2+Z_BZ_{2e}^2\right)Z_1\cos\theta_1\sin\theta_2\sin\theta_3\\-\left(Z_AZ_{3e}^2+2Z_BZ_1^2\right)Z_{2e}\sin\theta_1\cos\theta_2\sin\theta_3\\+j\left(\begin{array}{l}(Z_{2e}Z_{3e}+2Z_AZ_B)\,Z_1Z_{3e}\cos\theta_1\cos\theta_2\sin\theta_3\\-\left(Z_{2e}^2Z_AZ_B+2Z_1^2Z_{3e}^2\right)\sin\theta_1\sin\theta_2\sin\theta_3\\+\left(Z_{2e}^2+2Z_AZ_B\right)Z_1Z_{3e}\cos\theta_1\sin\theta_2\cos\theta_3\\+\left(2Z_1^2+Z_AZ_B\right)Z_{2e}Z_{3e}\sin\theta_1\cos\theta_2\cos\theta_3\end{array}\right)\end{array}\right)} \tag{16}$$

$$S_{22o}=\frac{\left(\begin{array}{l}\left(RZ_B-2Z_{3o}^2\right)Z_{2o}\sin\theta_2\sin\theta_3-RZ_BZ_{3o}\cos\theta_2\cos\theta_3\\+j\left(\left(R-2Z_B\right)Z_{2o}Z_{3o}\sin\theta_2\cos\theta_3+RZ_{3o}^2\cos\theta_2\sin\theta_3\right)\end{array}\right)}{\left(\begin{array}{l}RZ_BZ_{3o}\cos\theta_2\cos\theta_3-\left(RZ_B+2Z_{3o}^2\right)Z_{2o}\sin\theta_2\sin\theta_3\\+j\left(\left(R+2Z_B\right)Z_{2o}Z_{3o}\sin\theta_2\cos\theta_3+RZ_{3o}^2\cos\theta_2\sin\theta_3\right)\end{array}\right)} \tag{17}$$

3. SIMPLIFIED DESIGN PARAMETERS AND SPECIAL CASES

In order to simplify design parameters, we assume $Z_A = Z_B = Z_0$, $\theta_1 = \theta_2 = \theta_3 = \theta$, then (4), (5) and (9), (10) are simplified as (18):

$$\begin{cases}Z_1Z_{2e}Z_{3e}+\left[\left(2Z_1^2-Z_{2e}^2\right)Z_{3e}+\left(2Z_1^2-Z_{3e}^2\right)Z_{2e}\right.\\\left.+\left(Z_{2e}^2-2Z_{3e}^2\right)Z_1\right]\tan^2\theta=0\\\left(2Z_1^2Z_{3e}^2-Z_{2e}^2\right)\tan^2\theta+Z_{2e}Z_{3e}+2Z_1Z_{3e}+2Z_1Z_{2e}\\-2Z_1^2Z_{2e}Z_{3e}-Z_1Z_{2e}^2Z_{3e}-Z_1Z_{2e}Z_{3e}^2=0\\\left(R-2Z_{3o}^2\right)Z_{2o}\tan^2\theta-RZ_{3o}=0\\R=\dfrac{2Z_{2o}}{Z_{2o}+Z_{3o}}\end{cases} \tag{18}$$

To ensure that the above equations can be satisfied simultaneously at both frequencies f_1 and $f_2 = mf_1$, $m \geq 1$ (m is the frequency ratio), and to design compact power divider, the corresponding electrical lengths of each section at the frequencies f_1 and f_2 can be expressed as [32]:

$$\begin{cases} \theta_{f1} = \dfrac{\pi}{1+m} \\ \theta_{f2} = \dfrac{m\pi}{1+m} \end{cases} \tag{19}$$

Because the traditional microstrip transmission line is a special case of coupled-line, this proposed generalized power divider can be reduced four special cases power dividers. These special cases are summarized as follows (**Case A** to **Case D**).

3.1. Case A

When $Z_{2e} = Z_{2o} = Z_2$ and $Z_{3e} = Z_{3o} = Z_3$, this two-section coupled-line become two traditional microstrip transmission lines, the structure employs transmission line extensions at each port of the conventional Wilkinson power divider. In this approach, all three ports of the power divider have extensions for the dual-band operation without any coupling between them. The design Equation (18) become (20), this is a closed-form design, four Equation (20) and four free magnitudes (Z_1, Z_2, Z_3, R),these results have been published in [9] is a special case of this generalized power divider.

3.2. Case B

When only $Z_{2e} = Z_{2o} = Z_2$, one coupled-line becomes traditional microstrip transmission line, two output ports extended and coupled through a coupled-line section and the input port extension through a transmission line. The design Equation (18) become (21), solving these nonlinear design equations, the design parameters are calculated. This structure similar [26], but has the input port extension. Two examples (Example B1-Example B2) with different frequency-ratios are designed and simulated, and the detailed design parameters are listed in Table 1. The amplitude responses of S-parameters over different frequency ranges are shown in Figure 3. Obviously, ideal return loss of each port and isolation between output ports are attained, with insertion loss of 3.01 dB at two desired frequencies simultaneously in these two examples.

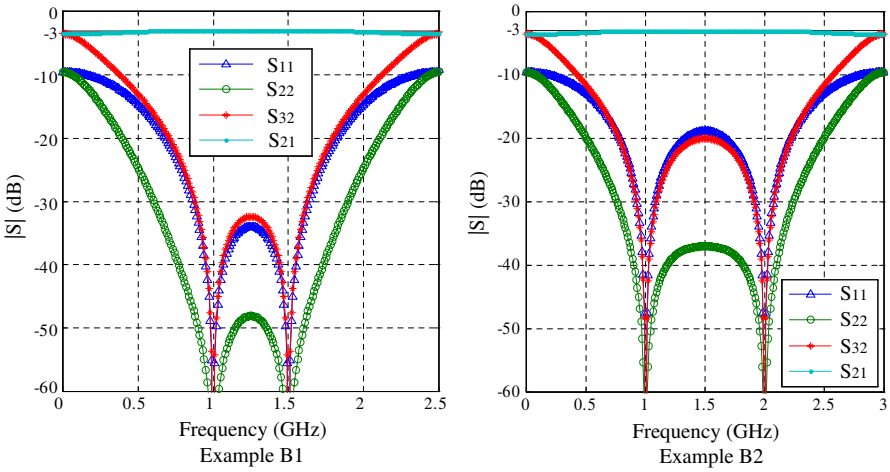

Figure 3. The amplitude responses of S-parameters of Example B1 and Example B2 in Case B.

Table 1. Final design parameters of three cases.

	f_1=1 GHz, $Z_A = Z_B = Z_0$=50 Ω					
	Case B		**Case C**		**Case D**	
	Example B1 m=1.5	**Example B2 m=2**	**Example C1 m=2.5**	**Example C2 m=3.5**	**Example D1 m=1.5**	**Example D2 m=2.5**
θ (rad) @ f_1	π/2.5	**π/3**	**π/3.5**	π/4.5	**π/2.5**	π/3.5
Z_1 (Ω)	47.83	**49.87**	**21.53**	13.99	**60.07**	82.62
Z_{2e} (Ω)	76.84	**79.09**	**48.81**	63.44	**110.63**	98.28
Z_{2o} (Ω)	76.84	**79.09**	**40.22**	36.23	**89.85**	89.11
Z_{3e} (Ω)	57.95	**62.90**	**28.41**	19.52	**72.70**	109.15
Z_{3o} (Ω)	39.52	**37.73**	**28.41**	19.52	**40.51**	36.29
R (Ω)	66.04	**67.71**	**58.61**	64.99	**68.93**	71.07

3.3. Case C

When only $Z_{3e} = Z_{3o} = Z_3$, one coupled-line becomes traditional microstrip transmission line, and the structure employs transmission line extension at each port of the coupled-line power divider. The design Equation (18) become (22), and solving these nonlinear design

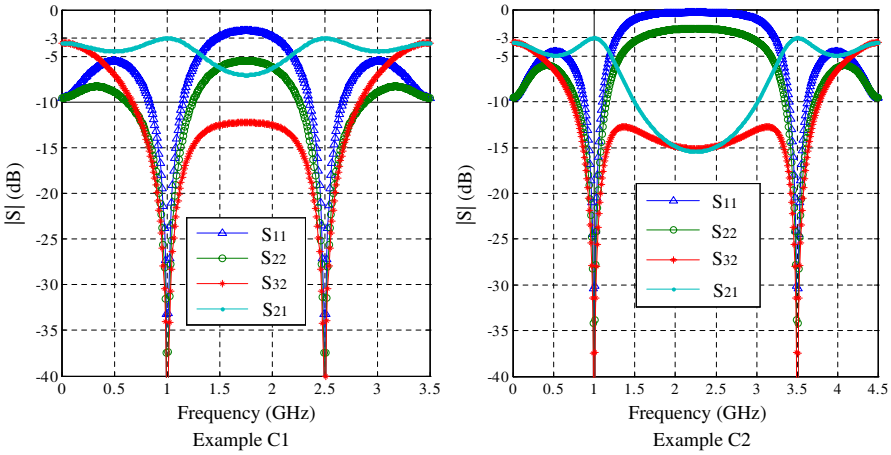

Figure 4. The amplitude responses of S-parameters of Example C1 and Example C2 in Case C.

Equation (22), the design parameters are calculated. Two examples (Example C1-Example C2) with different frequency-ratios are designed and simulated, and the detailed design parameters are listed in Table 1. The amplitude responses of S-parameters over different frequency ranges are shown in Figure 4. In these examples, ideal matching of each port, isolation between output ports, and insertion loss of 3.01 dB are satisfied at two desired frequencies simultaneously.

3.4. Case D

When the generalized coupled-line power divider with extended ports has two section coupled-lines, one conventional transmission line and an isolation resistor, the nonlinear design equations are (18), which has compact structure and flexible design parameters, solving nonlinear design Equation (18) by optimization algorithms, the design parameters are obtained. Two examples (Example D1-Example D2) with different frequency-ratios are designed and simulated, and the detailed design parameters are listed in Table 1. The amplitude responses of S-parameters over different frequency ranges are shown in Figure 5. The matching of both the input port and output ports at two frequencies is ideal, isolation between output ports at two frequencies is perfect, and the insertion loss equals to 3.01 dB at two desired frequencies simultaneously. In addition, when the frequency-ratio is relatively small, these generalized power dividers can be used as wideband ones, such as Example B1, Example B2 and Example D1.

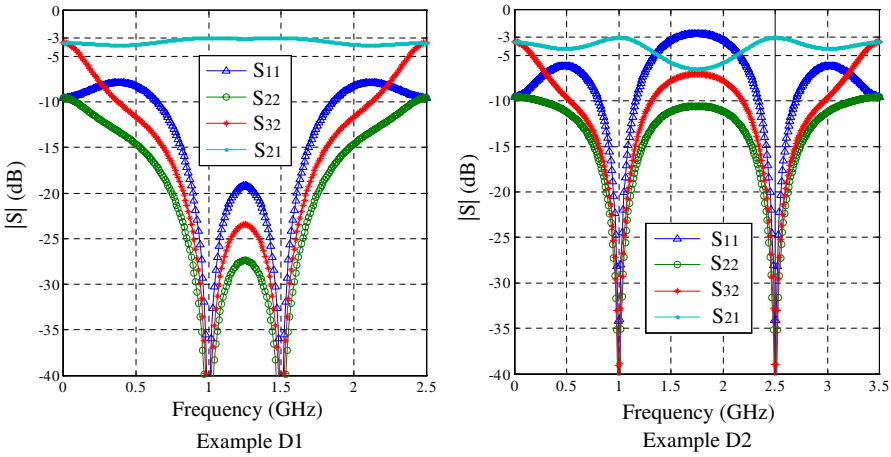

Figure 5. The amplitude responses of S-parameters of Example D1 and Example D2 in Case D.

Moreover, we need to indicate is that the simulated transmission line and coupled-line using ideal no-loss transmission line and coupled-line in the above cases.

$$\begin{cases} Z_1Z_2Z_3 + [2Z_1Z_3(Z_1 - Z_3) + 2Z_1Z_2(Z_1 + Z_2) \\ -Z_2Z_3(Z_2 + Z_3)]\tan^2\theta = 0 \\ \left(2Z_1^2Z_3^2 - Z_2^2\right)\tan^2\theta + Z_2Z_3 + 2Z_1Z_3 + 2Z_1Z_2 - 2Z_1^2Z_2Z_3 \\ - Z_1Z_2^2Z_3 - Z_1Z_2Z_3^2 = 0 \\ \left(R - 2Z_3^2\right)Z_2\tan^2\theta - RZ_3 = 0 \\ R = \dfrac{2Z_2}{Z_2 + Z_3} \end{cases} \tag{20}$$

$$\begin{cases} Z_1Z_2Z_{3e} + \left[\left(2Z_1^2 - Z_2^2\right)Z_{3e} + \left(2Z_1^2 - Z_{3e}^2\right)Z_2 + \left(Z_2^2 - 2Z_{3e}^2\right)Z_1\right]\tan^2\theta = 0 \\ \left(2Z_1^2Z_{3e}^2 - Z_2^2\right)\tan^2\theta + Z_2Z_{3e} + 2Z_1Z_{3e} + 2Z_1Z_2 - 2Z_1^2Z_2Z_{3e} \\ - Z_1Z_2^2Z_{3e} - Z_1Z_2Z_{3e}^2 = 0 \\ \left(R - 2Z_{3o}^2\right)Z_2\tan^2\theta - RZ_{3o} = 0 \\ R = \dfrac{2Z_2}{Z_2 + Z_{3o}} \end{cases} \tag{21}$$

$$\begin{cases} Z_1 Z_{2e} Z_3 + \left[\left(2Z_1^2 - Z_{2e}^2\right) Z_3 + \left(2Z_1^2 - Z_3^2\right) Z_{2e} + \left(Z_{2e}^2 - 2Z_3^2\right) Z_1\right] \tan^2\theta = 0 \\ \left(2Z_1^2 Z_3^2 - Z_{2e}^2\right) \tan^2\theta + Z_{2e} Z_3 + 2Z_1 Z_3 + 2Z_1 Z_{2e} - 2Z_1^2 Z_{2e} Z_3 \\ - Z_1 Z_{2e}^2 Z_3 - Z_1 Z_{2e} Z_3^2 = 0 \\ \left(R - 2Z_3^2\right) Z_{2o} \tan^2\theta - R Z_3 = 0 \\ R = \dfrac{2Z_{2o}}{Z_{2o} + Z_3} \end{cases} \tag{22}$$

3.5. Comparison of Four Special Cases

In order to compare the performance of proposed power divider with four cases at the same frequency ratio, we have designed four power dividers Case 1, Case 2, Case 3 and Case 4, and corresponding to the four cases Case A, Case B, Case C and Case D, respectively. Without loss of generalization, here, assume that the frequency ratio $m = 2.3$, $f_1 = 1.0\,\text{GHz}$, not a special value. So, four power dividers are working at 1 GHz/2.3 GHz, the detailed design parameters are listed in Table 2. The amplitude responses of S-parameters at the same frequency ranges with four cases are shown in Figure 6. Moreover, we need to indicate is that the simulated transmission line and coupled-line using ideal no-loss transmission line and coupled-line too.

From the simulation results we can see that, the performance of Case 2 is the best in the whole frequency range, the other three cases very close. However, compared with Case A with conventional transmission lines, Case B-Case D with coupled-line has advantages, such as compact structure and flexible design parameters due to introducing even- and odd-mode impedances.

Table 2. The design parameters of four cases.

	$f_1 = 1\text{GHz}$, $Z_A = Z_B = Z_0 = 50\,\Omega$, $m = 2.3$			
	Case A	Case B	Case C	Case D
	Case 1	Case 2	Case 3	Case 4
θ (rad) @ f_1	$\pi/2.3$	$\pi/2.3$	$\pi/2.3$	$\pi/2.3$
$Z_1\,(\Omega)$	24.28	52.99	23.14	79.61
$Z_{2e}\,(\Omega)$	47.20	79.87	45.49	106.17
$Z_{2o}\,(\Omega)$	47.20	79.87	40.67	89.28
$Z_{3e}\,(\Omega)$	31.50	68.88	30.01	103.28
$Z_{3o}\,(\Omega)$	31.50	36.35	30.01	37.29
$R\,(\Omega)$	59.98	68.72	57.55	70.54

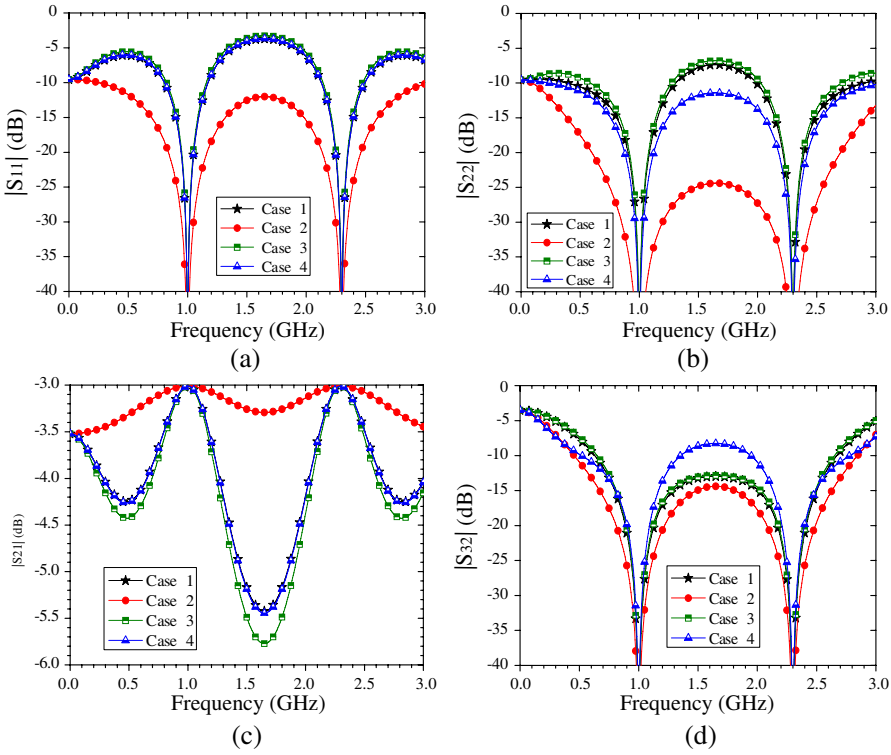

Figure 6. The amplitude responses of S-parameters of Case 1-Case 4.

4. EXPERIMENTAL RESULTS

In this section, to certify this structure and design parameters, a Case B power divider operates at 1 GHz and 2 GHz, a Case C power divider operates at 1 GHz and 2.5 GHz, and a Case D power divider operates at 1 GHz and 1.5 GHz are fabricated in microstrip technology, respectively. The design parameters are obtained from Example B2, Example C1 and Example D1 in Table 1, which is given in Section 3. In these three examples, a practical substrate with the relative dielectric constant of 2.55 and the height of 1 mm is applied. And the final photographs of the fabricated power dividers are shown in Figure 7, all the measured results shown in Figure 8 are collected from Agilent N5230C network analyzer.

The measured S-parameters of the Example B2 dual-band power divider are presented in Figure 8(a). It shows excellent performance with the insertion loss of 3.07 dB and 3.17 dB at two desired frequencies

simultaneously, return loss and isolation better than −15 dB from 0.73 to 2.4 GHz, the power divider can be used as wideband.

From Figure 8(b), in this Example C1 dual-band power divider, the absolute value of transmission parameters S_{21} is 3.12 dB and 3.37 dB at two desired frequencies simultaneously, the output matching parameters S_{22} and the isolation S_{32} are below 30 dB, but the input matching parameters S_{11} has a little frequency shift at 2.5 GHz.

From Figure 8(c), the transmission parameters S_{21} is approximately 3.02 dB and the corresponding values are 3.025 dB and 3.018 dB at 1 GHz and 1.5 GHz, the good isolation between the output ports S_{32},

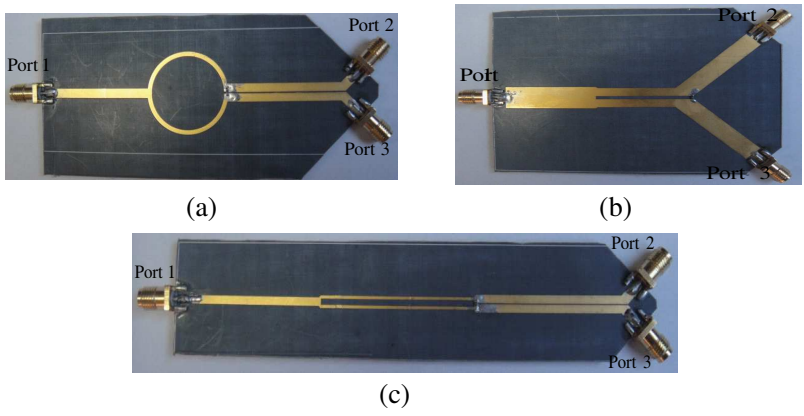

Figure 7. Photographs of the fabricated power dividers (Example B2, Example C1 and Example D1). (a) Example B2. (b) Example C1. (c) Example D1.

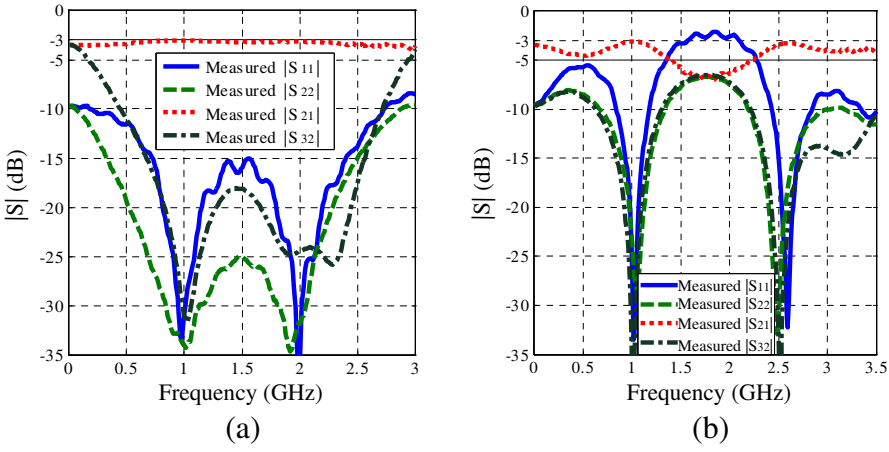

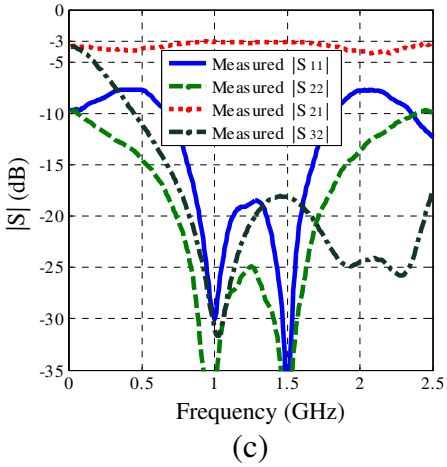

(c)

Figure 8. The measured S-parameters of the dual-band power dividers (Example B2, Example C1 and Example D1). (a) Example B2. (b) Example C1. (c) Example D1.

the input matching S_{11} and the output matching S_{22} are below -15 dB from 0.82 to 1.68 GHz, the power divider can be used as wideband too.

5. CONCLUSION

A generalized coupled-line power divider with extended ports for dual band has been proposed, analyzed, designed, and implemented in this paper. The power divider employs transmission line or coupled-lines extensions at each port. The design equations have been obtained by using rigorous even- and odd-mode analysis, and analytical ideal closed-form scattering parameter expressions are derived. Because the traditional microstrip transmission line is a special case of coupled-line, the proposed power divider can be regarded as a generalized model, which combines the dual-frequency modified Wilkinson power divider [9] and other three special cases have discussed above. The analytical design process is verified by experiments including three examples with different structures and frequency-ratios. The results of practical microstrip power dividers indicate that it can operate at desired dual-band with good performances in return loss, equal power dividing and isolation. Actually, this proposed power divider is very suitable for the microstrip circuit implementation in dual-band wireless systems.

ACKNOWLEDGMENT

This work was supported in part by National Natural Science Foundation of China (No. 61001060), the Fundamental Research Funds for the Central Universities (No. 2012RC0301), and Important National Science & Technology Specific Projects (No. 2010ZX03007-003-04). The authors would also like to thank the reviewers of this paper for their valuable comments and suggestions, which highly improved its overall quality.

REFERENCES

1. Wilkinson, E., "An N-way hybrid power divider," *IRE Trans. on Microw. Theory and Tech.*, Vol. 8, No. 1, 116–118, 1960.
2. Monzon, C., "A small dual-frequency transformer in two sections," *IEEE Trans. on Microw. Theory and Tech.*, Vol. 51, No. 4, 1157–1161, 2003.
3. Wu, L., Z. Sun, H. Yilmaz, and M. Berroth, "A dual-frequency Wilkinson power divider," *IEEE Trans. Microw. Theory Tech.*, Vol. 54, No. 1, 278–284, 2006.
4. Wu, Y., Y. Liu, and S. Li, "Unequal dual-frequency Wilkinson power divider including series resistor-inductor-capacitor isolation structure," *IET Microwaves, Antennas & Propagation*, Vol. 3, No. 7, 1079–1085, 2009.
5. Kawai, T., Y. Nakashima, Y. Kokubo, and I. Ohta, "Dual-band Wilkinson power dividers using a series RLC circuit," *IEICE Trans. on Electron.*, Vol. E91-C, No. 11, 1793–1797, 2008.
6. Wu, Y, Y. Liu, and S. Li, "An unequal dual-frequency Wilkinson power divider with optional isolation structure," *Progress In Electromagnetics Research*, Vol. 91, 393–411, 2009.
7. Cheng, K.-K. M. and C. Law, "A novel approach to the design and implementation of dual-band power divider," *IEEE Trans. on Microw. Theory and Tech.*, Vol. 56, No. 2, 487–492, 2008.
8. Wu, Y. L., Y. A. Liu, S. L. Li, and C. P. Yu, "A new symmetric modified Wilkinson power divider using L-type dual-band impedance matching structure," *Journal of Electromagnetic Waves and Applications*, Vol. 23, Nos. 17–18, 2351–2362, 2009.
9. Park, M. J. and B. Lee, "Wilkinson power divider with extended ports for dual-band operation," *Electronics Letters*, Vol. 44, No. 15, 916–917, 2008.
10. Li, J. C., J. C. Nan, X. Y. Shan, and Q. F. Yan, "A novel modified dual-frequency Wilkinson power divider with open stubs

and optional isolation," *Journal of Electromagnetic Waves and Applications*, Vol. 24, No. 16, 2223–2235, 2010.

11. Wu, Y., Y. Liu, and S. Li, "Dual-band modified Wilkinson power divider without transmission line stubs and reactive components," *Progress In Electromagnetics Research*, Vol. 96, 9–20, 2009.
12. Wu, Y., Y. Liu, Y. Zhang, J. Gao, and H. Zhou, "A dual band unequal Wilkinson power divider without reactive components," *IEEE Trans. on Microw. Theory and Tech.*, Vol. 57, No. 1, 216–222, 2009.
13. Huang, W., C. Liu, L. Yan, and K. Huang, "A miniaturized dual-band power divider with harmonic suppression for GSM applications," *Journal of Electromagnetic Waves and Applications*, Vol. 24, No. 1, 81–91, 2010.
14. Eccleston, K. W. and J. Zong, "Implementation of a microstrip square planar N-way metamaterial power divider," *IEEE Trans. on Microw. Theory and Tech.*, Vol. 57, No. 1, 189–195, 2009.
15. Wu, Y., Y. Liu, S. Li, C. Yu, and X. Liu, "Closed-form design method of an N-way dual-band Wilkinson hybrid power divider," *Progress In Electromagnetics Research*, Vol. 101, 97–114, 2010.
16. Rozzi, T., A. Morini, G. Venanzoni, and M. Farina, "Full-wave analysis of N-way power dividers by eigenvalue decomposition," *IEEE Trans. on Microw. Theory and Tech.*, Vol. 57, No. 5, 1156–1162, 2009.
17. Wu, Y., Y. Liu, Q. Xue, S. Li, and C. Yu, "Analytical design method of multi-way dual-band planar power dividers with arbitrary power division," *IEEE Trans. on Microw. Theory and Tech.*, Vol. 58, No. 12, 3832–3841, 2010.
18. Chen, H. and Y.-X. Zhang, "A novel compact planar six-way power divider using folded and hybrid-expanded coupled lines," *Progress In Electromagnetics Research*, Vol. 76, 243–252, 2007.
19. Al-Zayed, A. S. and S. F. Mahmoud, "Seven ports power divider with various power division ratios," *Progress In Electromagnetics Research*, Vol. 114, 383–393, 2011.
20. Lin, Z. and Q.-X. Chu, "In-/reverse-phase dual band power divider with variable division ratio," *Journal of Electromagnetic Waves and Applications*, Vol. 24, Nos. 14–15, 1897–1907, 2010.
21. Sun, Z. Y., L. J. Zhang, Y. P. Yan, and H. W. Yang, "Design of unequal dual-band gysel power divider with arbitrary termination resistance," *IEEE Trans. on Microw. Theory and Tech.*, Vol. 59, No. 8, 1955–1962, 2011.
22. Shamaileh, K. A. A., A. M. Qaroot, and N. I. Dib, "Non-uniform

transmission line transformers and their application in the design of compact multi-band bagley power dividers with harmonics suppression," *Progress In Electromagnetics Research*, Vol. 113, 269–284, 2011.

23. Chu, Q.-X., F. Lin, Z. Lin, and Z. Gong, "Novel design method of tri-band power divider," *IEEE Trans. on Microw. Theory and Tech.*, Vol. 59, No. 9, 2221–2226, 2011.
24. Tang, X. and K. Mouthaan, "Analysis and design of compact two-way Wilkinson power dividers using coupled lines," *Asia Pacific Microw. Conf.*, 1319–1322, Dec. 7–10, 2009.
25. Park, M.-J., "Two-section cascaded coupled line Wilkinson power divider for dual-band applications," *IEEE Microw. Wireless Compon. Lett.*, Vol. 19, No. 4, 188–190, 2009.
26. Park, M.-J., "Dual-band Wilkinson divider with coupled output port extensions," *IEEE Trans. on Microw. Theory and Tech.*, Vol. 57, No. 9, 2232–2237, 2009.
27. Wu, Y., Y. Liu, and Q. Xue, "An analytical approach for a novel coupled-line dual-band Wilkinson power divider," *IEEE Trans. on Microw. Theory and Tech.*, Vol. 59, No. 2, 286–294, 2011.
28. Lin, Z. and Q.-X. Chu, "A novel approach to the design of dual-band power divider with variable power dividing ratio based on coupled-lines," *Progress In Electromagnetics Research*, Vol. 103, 271–284, 2010.
29. Li, B., X. Wu, N. Yang, and W. Wu, "Dual-band equal/unequal Wilkinson power dividers based on coupled-line section with short-circuited stub," *Progress In Electromagnetics Research*, Vol. 111, 163–178, 2011.
30. Park, M.-J., "Coupled line Gysel power divider for dual-band operation," *Electronics Letters*, Vol. 47, No. 10, 599–601, 2011.
31. Wu, Y. and Y. Liu, "An unequal coupled-line Wilkinson power divider for arbitrary terminated impedances," *Progress In Electromagnetics Research*, Vol. 117, 181–194, 2011.
32. Wu, Y., Y. Liu, and X. Liu, "Dual-frequency power divider with isolation stubs," *Electronics Letters*, Vol. 44, No. 24, 1407–1408, 2008.